JOURNAL OF CATALYSIS **116**, 61–70 (1989)

Thermal Desorption–Infrared Study of Carbon Monoxide Adsorption by Alumina-Supported Platinum

ROGER BARTH,[1] RANGASAMY PITCHAI,* RUSSELL L. ANDERSON,*
AND XENOPHON E. VERYKIOS†

*Department of Chemistry, West Chester University, West Chester, Pennsylvania 19383; *Department of Chemical Engineering, Drexel University, Philadelphia, Pennsylvania 19104; and †Institute of Chemical Engineering and High Temperature Chemical Processes, Department of Chemical Engineering, University of Patras, Patras, Greece*

Received August 30, 1988; revised October 21, 1988

The thermal desorption of carbon monoxide from alumina-supported platinum has been studied by monitoring of the infrared spectrum of adsorbed CO as the temperature is increased. For the 0.5, 1, 2, and 10 wt% Pt samples studied, the areas of the peaks in the linear region increased with temperature until 100°C, whereupon they decreased steadily, reaching zero at about 400°C. The rate of disappearance of linearly adsorbed CO had two maxima, one at about 150°C and the other at about 250°C. The 0.5, 1, and 2% samples, which were fully dispersed, all displayed a peak at 2060 cm^{-1}, with a shoulder at about 2078 cm^{-1}. The 10% sample, which was 75% dispersed, had its main peak at 2083 cm^{-1} with a shoulder at 2069 cm^{-1}. For all samples, these peaks shifted to lower frequency as the temperature increased. The 2083 cm^{-1} peak is attributed to CO linearly adsorbed on Pt crystal faces, whereas the 2060 cm^{-1} peak is attributed to CO adsorbed by Pt particles that do not have extended crystal faces.

INTRODUCTION

Supported metal catalysts, despite their long history of importance, have proven to be intractable to detailed characterization. Even such fundamental information as metal particle size (average and distribution) is difficult to obtain and subject to many biased errors (*1–4*). Infrared spectroscopy was brought to bear on this problem nearly 35 years ago (*5*), and has been used heavily ever since. The spectrum of adsorbed carbon monoxide has been of particular interest from a practical and theoretical point of view. Nonetheless, there is still controversy regarding the interpretation of infrared spectra of adsorbed carbon monoxide.

In recent years it has become possible to measure vibrational spectra of carbon monoxide adsorbed by bulk platinum, either by reflection–absorption infrared spectroscopy (RAIR or IRAS) (*6–13*) or by electron energy loss spectroscopy (EELS) (*14–16*). This has made it possible to determine the vibrational spectrum of carbon monoxide on particular crystal faces of platinum. These data, in conjunction with other techniques applicable to bulk samples, especially temperature-programmed desorption (TPD or TDS) (*17*), are much less complicated to interpret than those obtained from supported platinum. An important theme in current research in this field is to interpret CO spectra from supported platinum in the light of those from bulk platinum (*18, 19*).

The spectrum of CO adsorbed by oxide-supported platinum displays peaks at frequencies in the region 2040 to 2090 cm^{-1}, and, sometimes, by peaks in the region 1780 to 1860 cm^{-1}. The 2040 to 2090 cm^{-1} peaks are attributed to linear CO, that is, CO bound to a single platinum atom. The 1780 to 1860 cm^{-1} peaks are attributed to bridging CO, that is, CO bound to more than one platinum atom (*20*). The assignment of the bridged peaks had come under attack (*21*), but is now generally accepted.

---

[1] To whom correspondence should be addressed.

0021-9517/89 $3.00

The linear peak shifts to higher frequency with increasing surface coverage (*22–28*). Two mechanisms have been put forward to account for this shift. One involves competition between adsorbed CO molecules for back-bonding metal *d* electrons (*21*). The other involves intermolecular vibrational coupling (*22–30*). There is evidence that the frequency of the linear band is an increasing function of platinum particle size (*31, 32*). This observation has been rationalized on the basis of competition for *d* electrons between metal–CO back-bonds and metal–metal bonds (*32*).

Table 1 summarizes vibrational spectroscopic studies of CO adsorbed by bulk platinum. Linear bands have been found at frequencies as low as 2065 cm^{-1} for low coverage at steps or kinks, and as high as 2107 cm^{-1} for full coverage on a flat (111) surface. It is interesting that the (111)-oriented polycrystalline ribbon gives a much lower CO stretching frequency at low coverage, and a much higher TPD maximum than any of the single crystal samples. As with supported platinum, the linear peak shifts to higher frequency with increasing surface coverage, a phenomenon that has been attributed to intermolecular vibrational coupling (*7*). Bridged CO, when observed, usually gives rise to bands in the 1840 to 1870 cm^{-1} region, although some lower frequencies have been noted and attributed to three and fourfold bridges (*8, 15*).

One of the complications of the strong interactions which CO molecules have with platinum and with one another is that the adsorbed layer is often nonuniform. This nonuniformity sometimes manifests itself in hysteresis in band position as a function of adsorbate dose (*6, 9*). In a convincing demonstration of nonuniform coverage on supported samples, it has been possible to measure spectra with peaks from both branches of the hysteresis (*33–35*). Nonuniformity can hamper efforts to vary surface coverage. The usual method for taking a series of spectra of a supported metal with different CO surface coverages is to admit measured

TABLE 1

Survey of IR and TPD Results for CO Adsorbed by Bulk Platinum

Surface	C–O frequency (cm^{-1})		Desorption maximum (K)	Technique	Comments	Reference
	Linear	Bridge				
(111)[a]	2065 → 2101[b]		750	RAIR[c]	Hysteresis in ν vs θ	(*6, 7*)
(111)	2089 → 2105	1855 → 1871	460	EELS[d]	$\nu_{\text{M-CO}}$ at 393 cm^{-1}	(*15*)
(111)	2079 → 2099			RAIR at 300 K		(*11*)
(111)	2107 → 2102			RAIR at 85 K		(*11*)
	2089 → 2091					(*11*)
(100)	2089 → 2093				Hysteresis 248 to 366 K	(*9*)
6(111) × (111)	2089 → 2105	1879	540, 440		Low bridge attributed to bottom of step (110)	(*15*)
		1694 → 1718		EELS		
4(111) × (100)	2065 → 2076		530, 410	RAIR at 85 K	Low band decreases at high θ	(*10, 12*)
	2086 → 2097					
(321)	2065 → 2095	1865	556, 436	RAIR	Kinked surface 3(111) × 2(100) × (111)	(*16*)
(410)	2072 → 2090			RAIR		(*13*)
(111)	2074 → 2110	1840 → 1870		RAIR	High bridge → twofold sites	(*8*)
		1810			Low bridge → threefold sites	
(432)	2080 → 2094		550, 420	RAIR	4(111) × 3(111) kinked	(*10*)
	2072 → 2077					

[a] Polycrystalline platinum; all others are single crystals.

[b] $x \rightarrow y$ represents change in frequency (ν) as one goes from low to high coverage (θ).

[c] Reflection absorption infrared spectroscopy.

[d] Electron energy loss spectroscopy.

doses of CO to an evacuated sample pellet. If adsorption is sufficiently fast and strong, the exterior regions of the pellet may be saturated while the interior regions remain bare (*36*). There are two approaches to circumvent this problem. In one approach the nonuniformly dosed sample is isolated and heated ("annealed") to a temperature at which the adsorbed CO can migrate freely; then cooled and studied at room temperature (*37*). Another approach is to saturate the entire sample with adsorbed CO and vary the coverage by desorption. An experimental realization of this approach is the thermal desorption–infrared spectroscopy technique that we have applied in this work.

The technique of thermal desorption–infrared spectroscopy (TD–IR) for adsorbates seems to have been developed by Miura and Gonzales (*38*), although there are a number of examples of similar techniques in the literature (*22, 39*). TD–IR was recently applied to supported platinum by Haaland (*19*). The technique can be applied in either of two methods. In the first method, adsorbate is admitted to the sample at a certain temperature, the sample is then subjected to continuous purging or evacuation, and the temperature is raised steadily as spectra are taken at intervals. In the second method, the adsorbate is admitted at some elevated temperature, the sample is subjected to purging or evacuation at constant temperature, and spectra are taken at intervals. The advantage of the second method is that a constant temperature provides a constant spectral background and hence produces more precise results. Nonetheless, we have chosen the first method, which has the advantage of revealing the low-temperature behavior of the adsorbate. Also, the experiments are much faster, the desorption taking about 3 h instead of 30 h.

Our objective in this paper is to present a detailed study of the influence of surface coverage on the adsorption of carbon monoxide under conditions that minimize the influence of nonuniform surface coverage. We have used samples similar in platinum content to practical alumina-supported catalysts. Another objective is to demonstrate the usefulness of the TD–IR technique for qualitative desorption studies of samples that are difficult to study with ordinary TPD (*40, 41*).

EXPERIMENTAL METHODS

Catalyst samples were prepared by adding the proper amount of an aqueous solution of chloroplatinic acid (5.035 wt% in platinum) to 10 g of the support material, aluminum oxide C (Degussa), and 150 ml of water in a beaker. The mixture was stirred at about 80°C until the liquid had evaporated, then put into a 110°C drying oven overnight. The resulting powder was packed into a stainless-steel tube and subjected to heating at 200°C in flowing nitrogen for 1 h and in flowing hydrogen for 5 h. It was then cooled in flowing nitrogen, unpacked, and stored. The blank alumina sample was prepared by wetting a quantity of support material and drying it at 120°C. This was necessary because of the very low bulk density of aluminum oxide C as supplied. The 10% Pt/Al_2O_3 sample had poor infrared transmission, so a diluted sample was used in infrared experiments. To prepare the diluted sample, 0.200 g of 10% Pt/Al_2O_3 was ground with 0.896 g of alumina, prepared as above, in a porcelain mortar and pestle.

Chemisorption experiments were conducted on a Micromeritics Accusorb 2100E surface analyzer. The catalyst samples were treated *in situ* three times with 104 to 109 kN/m^2 hydrogen at 200°C for about 1 h each time, then evacuated overnight. Hydrogen adsorption was conducted at room temperature with dosing pressures ranging from 6.7 to 54 kN/m^2. H/Pt ratios were determined by extrapolating the high-pressure end of the isotherm to zero pressure.

Samples for infrared spectroscopy were ground with a porcelain mortar and pestle, passed through a 120-mesh sieve, and pressed between glassine sheets at 35.6 kN in a 13-mm-diameter die. The pressed sample weighed between 20 and 30 mg. The resulting self-supporting disk was mounted in a quartz sample holder, which was placed in an infrared cell. The cell was based on a design of Kokes *et al.* (*42*). It consisted of a quartz tube to which brass end rings had been mounted with epoxy cement. Viton O-rings provided a gastight seal between removable sodium chloride windows and the end rings. The seals were protected from high temperatures by cooling water which flowed through channels in the end rings. The windows were held in place against the sealing rings with brass retaining rings which screwed down over the windows and end rings. Two tubes fitted with PTFE stopcocks were sealed at right angles to and near the ends of the main quartz tube, serving to carry gases to and from the cell. A thermocouple, sheathed with stainless steel, was fed through a side arm in the outlet tube and sealed with epoxy cement. The end of the sheath, to which the junction was grounded, was in contact with the sample holder and served to position it reproducibly. The main tube of the cell was wrapped with heating tape and insulated. Infrared studies were carried out with a Perkin–Elmer Model 1750 Fourier transform instrument equipped with a DTGS detector.

Gases were fed to the cell via a gas switching and purification system. The lines from the gas tanks to the system were polyethylene, the lines in the system were copper, and the fittings were brass. The system was connected to the cell by a flexible braided stainless-steel line and an Ultratorr (Cajon), fitting. Helium and hydrogen passed through traps containing (1) activated Oxy-absorbent (Alltech Associates), (2) activated zeolite 3A, and (3) activated 10% MnO_x/Cab-O-Sil. The Oxy-absorbent and zeolite traps were type 304 stainless steel; the MnO_x traps were glass. Carbon monoxide was passed through an activated zeolite 3A trap, and oxygen was used as supplied. Gases were of standard grade and were supplied by Airco.

At the beginning of each experimental run the catalyst was subjected to the following activation procedure:

1. Flowing oxygen at 400°C for 60 min.
2. Purging with helium at 400°C for about 10 min.
3. Flowing hydrogen at 400°C for 30 min.
4. Purging with helium at 400°C for about 10 min.
5. Flowing oxygen at 400°C for 90 min.
6. Purging with helium at 400°C for about 10 min.
7. Flowing hydrogen at 400°C for 90 min.
8. Cooling to 300°C in flowing hydrogen.
9. Flowing hydrogen at 300°C for 20 min.
10. Switch to flowing helium and cooling to room temperature.

Background spectra were taken at intervals of about 100°C during the final cooling step. The temperatures were maintained constant while each background spectrum was taken. Constant temperatures were maintained with a temperature controller. The programmed heating rate was maintained manually by adjusting a variable autotransformer. A fresh sample disk was pressed for each run.

The experiments proceeded as follows:

1. Activate sample as above.
2. Switch to carbon monoxide at room temperature for 5 min.
3. Purge with helium at room temperature for 5 min.
4. Program temperature at 2.5°C/min and take spectra every 10°C.

The helium flow rate during the temperature-programmed part of the run was maintained at 3.2 mmol/min, except as noted. The pressure in the cell was always 101 kPa.

Absorbance spectra were produced by comparing each spectrum to the background taken at the temperature nearest to that of the spectrum. The background was multiplied or divided by a constant factor to achieve a good match in the region 2250 to 1650 cm^{-1}. Then the difference routine was applied, which provided a net absorbance spectrum.

RESULTS

We have performed thermal desorption–infrared spectroscopic studies of carbon monoxide adsorption by alumina-supported platinum catalysts containing 0.5, 1, 2, and 10% platinum by weight. Characterization of these samples by hydrogen chemisorption, the results of which are presented in Table 2, shows that the 0.5, 1, and 2% samples are fully dispersed ($H/M \geq 1$), while the 10% sample is not fully dispersed ($H/M = 0.75$).

Figures 1–4 show spectra, recorded at different temperatures, of CO adsorbed by the 1% catalyst. The room-temperature spectrum displays a peak at 2060 cm^{-1}, with a shoulder at 2078 cm^{-1} and a broad peak at about 1800 cm^{-1}. For clarity, we refer to these peaks by their room-temperature positions. We might, for example, mention the 2060 cm^{-1} peak at 150°C, although the actual position of the peak at this temperature is 2048 cm^{-1}. Figure 1 shows that as the temperature increases to 100°C, the 2060 cm^{-1} peak increases in intensity and shifts to lower frequency, the 2078 cm^{-1} shoulder remains unchanged, and the 1800 cm^{-1} peak decreases in intensity and seems to split into two peaks at 1845 and 1785 cm^{-1}. Figure 2 shows that as the temperature increases to 180°C, the peaks at 2060 and 1800 cm^{-1} decline in intensity. The 2078 cm^{-1} shoulder seems to increase in intensity, although this change may be apparent only, as the shoulder moves closer to the main peak. Both linear (above 2000 cm^{-1}) peaks shift to lower frequency as the temperature increases. Figure 3 shows that from 190 to 240°C the 2078 cm^{-1} shoulder remains unchanged as the 2060 cm^{-1} peak continues to lose intensity and shift to lower frequency. At 250°C the 2078 cm^{-1} peak resumes its decline and shifts to lower frequency. At this temperature the removal of the 2060 cm^{-1} peak begins to reveal a broad peak centered at about 2000 cm^{-1}. Figure 4 shows that at temperatures above 280°C the linear peaks lose their identity, and only a single peak remains whose final frequency is 2040 cm^{-1}.

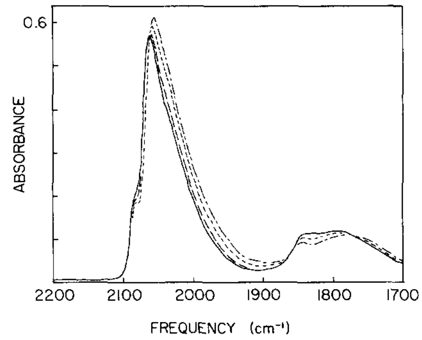

Fig. 1. IR spectra, CO on 1% Pt/Al_2O_3: —, 30°C; --, 50°C; ---, 70°C; ---, 90°C.

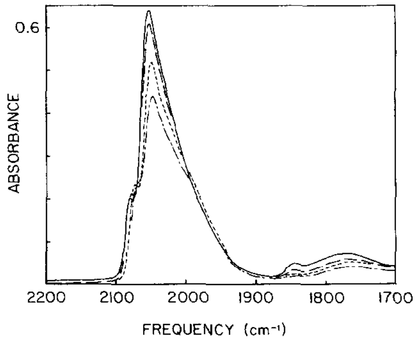

Fig. 2. IR spectra, CO on 1% Pt/Al_2O_3: —, 110°C; --, 130°C, ---, 150°C; ---, 170°C.

TABLE 2

Hydrogen Chemisorption Results

Pt content	H/Pt
0.5	1.20
1.0	1.29
2.0	1.26
10.0	0.75

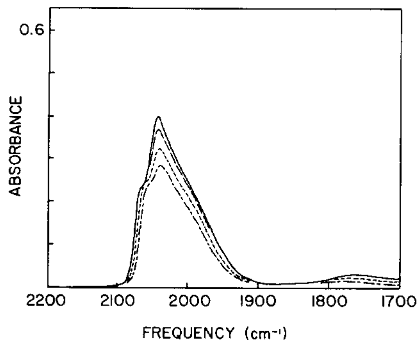

Fig. 3. IR spectra, CO on 1% Pt/Al$_2$O$_3$: —, 190°C; --, 210°C; ---, 230°C; – – –, 250°C.

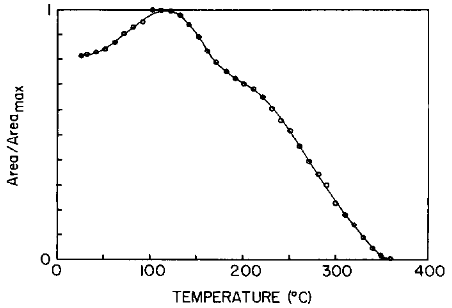

Fig. 5. Linear peak areas versus temperature, 1% Pt/Al$_2$O$_3$.

The changes in integrated intensity for the linear region, from 2120 to 1900 cm^{-1}, are illustrated graphically in Fig. 5 for the 1% sample. In this figure, we note that the area goes through a maximum at 110°C and declines monotonically thereafter, with breaks in the curve at about 150 and 220°C. Figure 6 shows plots of differences in the areas $(A_T - A_{T+5})$ versus temperature (T). These plots are, in effect, simulated temperature-programmed desorption curves. Each curve shows a minimum at 50–60°C representing the temperature of maximum intensity gain, and maxima at 120–150 and 250–300°C representing temperatures of maximum intensity loss. The lower maximum occurs at about 150°C for the 0.5 and 1% samples, and at about 130°C for the 2 and 10% samples.

Figure 7 shows the peak positions for linearly adsorbed CO on the 1% sample plotted against temperature. We caution the reader that the apparent positions of unresolved peaks can be significantly different from the true absorption maxima. The 2060 cm^{-1} peak shifts to lower frequency about at 0.1 cm^{-1}/K for the region from room temperature to 150°C, whereupon it remains at 2046 cm^{-1} until 200°C. At 200°C it continues to shift, although above about 260°C it becomes difficult to quantify its exact position. The 2078 cm^{-1} peak seems to remain at a constant frequency until 120°C, then it begins to shift to lower frequency. There seems to be a halt in the shift at about 200°C and 2067 cm^{-1}, but the difficulty of measuring the position of a shoulder which has no real maximum requires us to appeal to other data.

The spectra of CO adsorbed on 1% Pt/

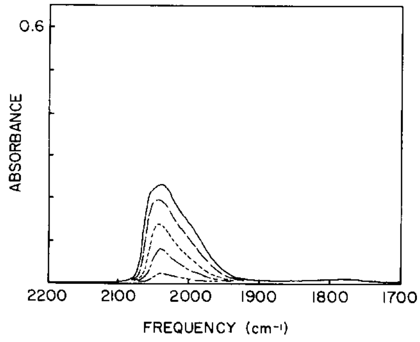

Fig. 4. IR spectra, CO on 1% Pt/Al$_2$O$_3$: —, 270°C; --, 290°C; ---, 310°C; – – –, 330°C; – – – –, 350°C.

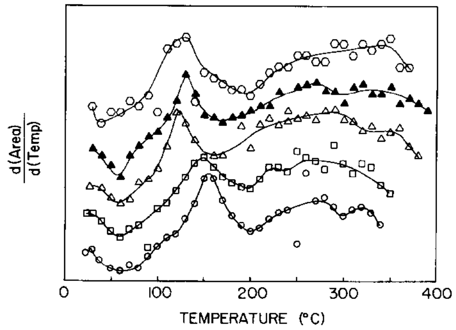

Fig. 6. Peak area derivatives: ○, 0.5% Pt; □, 1% Pt; △, 2% Pt; ▲, 2% Pt fast flow; ○, 10% Pt.

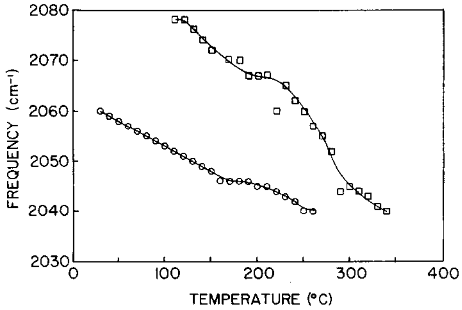

FIG. 7. Peak positions versus temperature, 1% Pt/Al$_2$O$_3$.

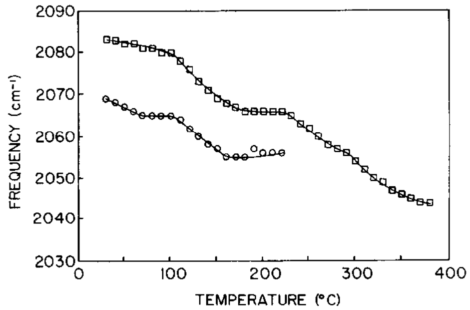

FIG. 9. Peak positions versus temperature, 10% Pt/Al$_2$O$_3$.

Al$_2$O$_3$ are essentially the same as those of CO adsorbed on 0.5% and 2% Pt/Al$_2$O$_3$, but differ from those of CO adsorbed on 10% Pt/Al$_2$O$_3$, some of which are shown in Fig. 8. At 30°C the 10% sample displays its main peak at 2083 cm^{-1} and a distinct shoulder at 2069 cm^{-1}. The shoulder becomes less distinct above 150°C, although we have attempted to follow it out to 220°C. The main peak is quite clear, and can easily be followed until it disappears above 380°C. If we identify the main peak on this sample with the shoulder on the 1% Pt/Al$_2$O$_3$ sample, and vice versa, then we can use the main peak positions for the 10% sample, shown in Fig. 9, to check the results for the shoulder positions of the 1% sample, shown in Fig. 7. Figure 9 unambiguously shows the halt at 200°C in the frequency shift of the higher peak which we had seen less clearly in Fig. 7. In addition, this figure seems to show a break in the curve at 100°C.

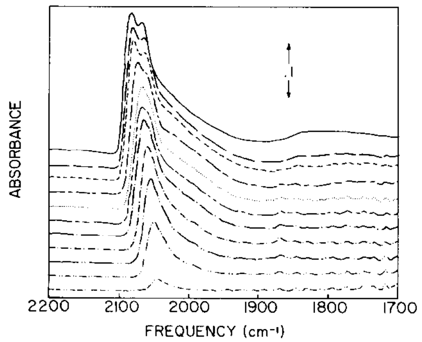

FIG. 8. IR spectra, CO on 10% Pt/Al$_2$O$_3$: —, 30°C; --, 70°C; ---, 100°C; ---, 130°C; · · ·, 170°C; ----, 200°C; -·-, 230°C; -··, 270°C; -··-, 300°C; -···, 330°C; --··--, 370°C.

In an effort to assess the influence of readsorption on these results, we performed a TD–IR experiment on the 2% Pt/Al$_2$O$_3$ with the helium flow rate increased by a factor of nearly 3 (to 9.1 mmol/min). As shown in Fig. 6, this did not affect the results significantly.

A sample of alumina without platinum, subjected to an abbreviated activation sequence, displayed no peaks in the region 2250 to 1650 cm^{-1} after exposure to CO and purging at room temperature.

DISCUSSION

Our results plainly show that TD–IR can reveal qualitative details in the desorption curve that traditional TPD cannot. In particular, we noted a sharp low-temperature maximum and a broad high-temperature maximum. These results are in rough agreement with TPD results for CO on bulk platinum, summarized in Table 1. The apparent tendency for the lower maximum to occur at lower temperature for the more heavily loaded samples suggests that the adsorption strength depends on particle size. Traditional TPD curves for CO adsorbed by supported platinum generally have a single very broad maximum (*40*), doubtless because of extensive readsorption. It is important to realize that there is no reason to suppose that the absorptivity of adsorbed

CO remains constant with surface coverage. Nor can it be assumed that all of the species giving rise to absorption in the linear region have the same absorptivity. Thus these curves are to be interpreted in a qualitative sense only.

One interesting result we report here is the increase in the integrated intensity of the peaks due to linearly adsorbed CO as the temperature increases from 30 to 100°C. As no additional CO is admitted to the system, there are only three possible explanations for this increase: either the absorptivity of some of the linearly adsorbed CO is enhanced, or CO which is not linearly adsorbed is converted to the linear form, or CO adsorbed by the support could migrate to the metal. This last explanation seems unlikely in that we did not observe any band attributable to CO adsorbed by alumina after room-temperature helium purging prior to temperature programming. Also, preliminary results on silica-supported platinum show a similar increase in the intensity of the linear peaks. Absorptivity enhancement might be rationalized by supposing that adsorbed molecules could migrate, under the influence of the increased temperature, to sites where their absorptivity is enhanced, for example, sites at steps (*43*). For migration to occur, there must be vacant sites. It is reasonable to suppose that some sites would be vacant after purging in light of Haaland's observation that alumina-supported platinum is not saturated with adsorbed CO, even at a CO partial pressure as high as 10 kPa (*19*). If we assume that all sites are occupied when the sample is treated with 101 kPa of CO at room temperature, we must infer that the absorptivity enhancement sites are vacated upon purging at low temperature, and are the sites of the most weakly held CO. But step sites are known to absorb CO more strongly than flat sites (*12, 13, 15, 16, 44*). In general, the idea of sites which adsorb CO weakly but which cause enhanced absorptivity seems implausible. Another explanation could be that absorptivity enhancement is due to a decrease in the local population of adsorbed CO. If the adsorbed CO is compressed into islands at low temperature, raising the temperature might cause relaxation into a less compressed layer with, perhaps, higher absorptivity. The absorptivity of linearly adsorbed CO has been observed to decrease with increasing coverage (*45*). Whether islands do, in fact, form at room temperature is still an open question (*23, 46*).

Another possible explanation for the increase in linear band intensity with temperature is that some of the bridged CO could be converted to the linear form. Figure 1 shows that the peaks in the bridge region do lose intensity as the temperature is raised, although we are reluctant to quantify this because the background in this region changes significantly in this temperature range. Conversion of bridged CO to linear CO could be due to a decrease in the local coverage. On the (111) surface of platinum, bridging is observed only at coverages in excess of 0.33, and it has been associated with a change in the structure of the adsorbed layer (*8, 14, 15, 47*). It is reasonable to suppose that when the local surface concentration of CO is decreased, the high-coverage type layer could relax to the low-coverage structure with concomitant conversion of bridged CO to the linear form. We offer this scenario as an example rather than as a specific mechanism. As we shall show, it is not always safe to generalize results from bulk platinum to supported platinum. The last explanation is the most plausible in that it accounts for the observed increase in linear band intensity and loss in bridge band intensity.

The frequency of the main peak for the fully dispersed samples (0.5, 1, and 2% Pt/Al_2O_3) cannot be accounted for on the basis of adsorption by platinum crystal faces. The C–O stretching frequency has been measured on the (111), (100), 6(111) × (111), 4(111) × (100), (321), and (410) faces of platinum; Table 1 summarizes the results. In no case has a peak as low as 2060 cm^{-1} been observed. At high coverage, all of these faces give rise to peaks between

2090 and 2110 cm^{-1}. We infer from this that the peak we observed at 2060 cm^{-1} which shifts to lower frequency at higher temperature is due to adsorption by platinum particles that do not have extended crystal faces, either because they are too small or because of their morphologies. The large displacement of the frequency of CO adsorbed by such particles compared to CO adsorbed by bulk platinum may be due to an intrinsic particle size effect or to a support effect. We have a preliminary indication that CO adsorbed by fully dispersed platinum on titania also gives rise to a peak at 2060 cm^{-1}, which suggests that the particle size is mainly responsible for the displacement.

The higher-frequency (2080 cm^{-1}) peak may well be due to adsorption on crystalline platinum. Its frequency lies in the range reported for linear adsorption on bulk platinum, and its intensity is markedly enhanced on the 10% Pt/Al_2O_3 sample, whose dispersion has been measured to be 75%. The presence of both peaks on all of our samples suggests that the platinum particle sizes are broadly distributed. On a commercial catalyst with a large (40 Å) average particle size, Haaland (*19*) reports a peak at 2075 cm^{-1} with a broad shoulder at about 2025 cm^{-1}. This is very similar to our observations, except that his sample does not display the 2060 cm^{-1} peak which we observe, suggesting that his sample does not contain significant amounts of very highly dispersed platinum. Also, we could not observe the 2025 cm^{-1} peak until 250°C, by which time it had shifted to 2000 cm^{-1}, although, in retrospect, we would note a tail on the 2060 cm^{-1} peak, visible in Fig. 8, may well be the 2025 cm^{-1} peak observed by Haaland.

Haaland has attributed the peak at 2025 cm^{-1} to adsorption on steps. RAIR and EELS studies on bulk platinum lend little support to this assignment. On Pt 6(111) × (111) Hopster and Ibach (*15*) reported, on the basis of EELS studies, that CO adsorbed at both steps and terraces had a frequency of 2089 cm^{-1}. On Pt 4(111) × (100), Hayden *et al.* reported a frequency of 2065 cm^{-1}, shifting to 2076 with increasing coverage, for CO adsorbed at steps (*12*). The peak at 2025 cm^{-1}, shifting lower on desorption, seems too low in frequency to be identified with adsorption on steps. It seems more likely that this peak is due to adsorption of CO by sites not found on extended crystals. Such sites could be corners or sites in the vicinity of electrically active centers on the support.

Like Haaland, we see two peaks in the bridge region, one at 1845 cm^{-1} and the other at 1760 to 1780 cm^{-1}. Haaland assigns the higher peak to CO in twofold bridge sites, and the lower peak to CO in threefold hollow sites. The frequency of the higher peak is in good agreement with the 1840–1857 cm^{-1} measured by Hayden and Bradshaw (*8*) using RAIR on Pt(111), but the lower peak differs from the 1810 cm^{-1} peak which they measured. Because of interference from water vapor, it is difficult to get precise results from either transmission or RAIR in this region of the spectrum. It is likely that when spectra with the detail attained by Hayden and Bradshaw are obtained on other crystal faces they will provide further enlightenment.

The shifting of the linear peaks to lower frequency with decreasing coverage is consistent with the literature. This has usually been interpreted as resulting from decreasing coupling among oscillating adsorbed CO molecules (*7, 22, 29*). A study of CO adsorption by Pt(111) at low temperature, in which two nonshifting bands were observed to change in relative intensity as the coverage changed (*11*), and one involving adsorption of a single CO molecule per particle (*30*) suggest that this interpretation may not be the whole story.

On the basis of this study we conclude that there are two thermal desorption maxima for CO adsorbed by alumina-supported platinum, one at 130 to 150°C and the other at about 250°C. We further conclude that the peak at 2080 cm^{-1} may be due to CO adsorption on a platinum crystal face. The peak at 2060 cm^{-1} is due to CO adsorbed by small platinum particles, and the peak at 2025 cm^{-1} may be due to CO adsorbed by platinum which interacts with the support. Neither the 2060 cm^{-1} peak nor the 2025 cm^{-1} peak can be attributed to CO adsorbed on crystal faces; these peaks have no analogs on bulk platinum.

ACKNOWLEDGMENT

This work was supported, in part, by grants from West Chester University.

REFERENCES

1. Dixon, L. T., Barth, R., Kokes, R. J., and Gryder, J. W., *J. Catal.* **37,** 376 (1975).
2. Matyi, R. J., Schwartz, L. H., and Butt, J. B., *Catal. Rev. Sci. Eng.* **29,** 41 (1987).
3. Crucq, A., Degols, L., Lienard, G., and Frennet, A., *Acta Chim. Sci. Hung.* **111,** 547 (1982).
4. Hall, D. I., Self, V. A., and Sermon, P. A., *J. Chem. Soc. Faraday Trans. 1* **83,** 2693 (1987).
5. Eischens, R. P., Pliskin, W. A., and Francis, S. A., *J. Chem. Phys.* **22,** 1786 (1954).
6. Shigeishi, R. A., and King, D. A., *Surf. Sci.* **58,** 379 (1976).
7. Crossley, A., and King, D. A., *Surf. Sci.* **68,** 528 (1977).
8. Hayden, B. E., and Bradshaw, A. M., *Surf. Sci.* **125,** 787 (1983).
9. Banholzer, W. F., and Masel, R. I., *Surf. Sci.* **137,** 339 (1984).
10. Greenler, R. G., Hayden, B. E., Kretzschmar, K., Klauser, R., and Bradshaw, A. M., *in* "Proceedings, 8th International Congress on Catalysis," Vol. 4, p. 197. Verlag Chemie, Weinheim, 1985.
11. Severson, M. W., Tornquist, W. J., and Overend, J., *J. Phys. Chem.* **88,** 469 (1984).
12. Hayden, B. E., Kretzschmar, K., Bradshaw, A. M., and Greenler, R. G., *Surf. Sci.* **149,** 394 (1985).
13. Banholzer, W. F., Parise, R. E., and Masel, R. I., *Surf. Sci.* **155,** 653 (1985).
14. Froitzheim, H., Hopster, H., Ibach, H., and Lehwald, S., *Appl. Phys.* **13,** 147 (1977).
15. Hopster, H., and Ibach, H., *Surf. Sci.* **77,** 109 (1978).
16. McClelland, M. R., Gland, J. L., and McFeeley, F. R., *Surf. Sci.* **112,** 63 (1981).
17. Collins, D. M., and Spicer, W. E., *Surf. Sci.* **69,** 85 (1977).
18. Greenler, R. G., Burch, K. D., Kretzschmar, K., Klauser, R., and Bradshaw, A. M., *Surf. Sci.* **152/153,** 338 (1985).
19. Haaland, D. M., *Surf. Sci.* **185,** 1 (1987).
20. Sheppard, N., and Nguyen, T. T., *Adv. Infrared Raman Spectrosc.* **5,** 67 (1978).
21. Blyholder, G., *J. Phys. Chem.* **68,** 2772 (1968).
22. Eischens, R. P., Francis, S. A., and Pliskin, W. A., *J. Phys. Chem.* **60,** 194 (1956).
23. Cant, N. W., and Donaldson, R. A., *J. Catal.* **78,** 461 (1982).
24. Haaland, D. M., and Williams, F. L., *J. Catal.* **76,** 450 (1982).
25. Palazov, A., Bonev, Ch., Kadinov, G., Shopov, D., Lietz, G., and Volter, J., *J. Catal.* **71,** 1 (1981).
26. Toolenaar, F. C. J. M., Stoop, F., and Ponec, V., *J. Catal.* **82,** 1 (1983).
27. Queau, R., and Poilbanc, R., *J. Catal.* **27,** 200 (1972).
28. Queau, R., Labroue, D., and Poilbanc, R., *J. Catal.* **69,** 249 (1981).
29. Hammaker, R. M., Francis, S. A., and Eischens, R. P., *Spectrochim. Acta* **21,** 1295 (1965).
30. Primet, M., de Menorval, L.-C., Fraissard, J., and Ito, T., *J. Chem. Soc. Faraday Trans. 1* **81,** 2867 (1985).
31. Dalla Betta, R. A., *J. Phys. Chem.* **79,** 2519 (1975).
32. Solomennikov, A. A., Lokhov, Yu. A., Davydov, A. A., and Ryndin, Yu. A., *Kinet. Katal.* **20,** 589 (1979).
33. Bartok, M., Sarkany, J., and Sitkei, A., *J. Catal.* **72,** 236 (1981).
34. Sarkany, J., Bartok, M., and Gonzalez, R. D., *J. Catal.* **81,** 347 (1983).
35. Sarkany, J., and Bartok, M., *J. Catal.* **92,** 388 (1985).
36. Eischens, R. P., *Acc. Chem. Res.* **5,** 74 (1972).
37. Palazov, A., Chang, C. C., and Kokes, R. J., *J. Catal.* **36,** 338 (1975).
38. Miura, H., and Gonzalez, R. D., *J. Phys. E* **15,** 373 (1982).
39. Griffin, G. L., and Yates, J. T., *J. Catal.* **73,** 396 (1982).
40. Herz, R. K., Kiela, J. B., and Marin, S. P., *J. Catal.* **73,** 66 (1982).
41. Huang, Y.-J., Xue, J., and Schwarz, J. A., *J. Catal.* **109,** 396 (1988).
42. Kokes, R. J., Dent, A. L., Chang, C. C., and Dixon, L. T., *J. Amer. Chem. Soc.* **94,** 4429 (1972).
43. Greenler, R. G., Dudeck, J. A., and Beck, D. E., *Surf. Sci.* **115,** L453 (1984).
44. Gdowski, G., and Madix, R. J., *Surf. Sci.* **115,** 524 (1982).
45. Sarkany, J., and Gonzalez, R. D., *Appl. Spectrosc.* **36,** 320 (1982).
46. Olsen, C. W., and Masel, R. I., *J. Vac. Sci. Technol. A* **6,** 792 (1988).
47. Ertl, G., Neumann, M., and Streit, K. M., *Surf. Sci.* **64,** 393 (1977).